

Energetics of the formation and migration of defects in Pb(110)

M. Karimi

Physics Department, Indiana University of Pennsylvania, Indiana, Pennsylvania 15705

G. Vidali

Physics Department, Syracuse University, Syracuse, New York 13244

I. Dalins

Marshall Space Flight Center, Huntsville, Alabama 35812

(Received 5 April 1993)

As part of our investigations on the disordering of metal surfaces, we report the results of our calculations of the energetics of formation and migration of defects in Pb(110) using molecular-dynamics and molecular-statics simulations. We used the embedded-atom method to describe the interatomic interactions. Defect formation and migration energies have been calculated at the surface as well as in the near-surface region. Vacancy, divacancy, and interstitial formation and migration energies converge to bulk values already at a few layers below the surface. Our results are compared with recent simulations of Cu and Ni and with experimental data. We also calculated the surface Debye temperature and surface energy. We find that the surface Debye temperature, surface single-vacancy formation energy, and surface divacancy formation energy are all lower than their bulk values. Our result for the surface energy is lower than the experimental values.

I. INTRODUCTION

Advances in computer-simulation techniques have reached a level of sophistication that they now can not only complement experiments but also predict new materials and perhaps dictate directions of material processing. In particular, computer simulations are very useful in the study of properties of systems where the low symmetry makes analytical calculations very difficult.¹⁻²³ This is the case, for example, of the study of properties of surfaces and defects near surfaces or in the bulk.

The first step in any atomistic computer simulation is the modeling of interatomic interactions. Current approaches range from empirical to ones derived from first-principles calculations. In empirical approaches, atoms are considered as point particles which interact with one another through some type of model potential chosen for its analytical convenience. On the other hand, in a first-principles approach, all of the complexities of the problem (electronic) are included in the calculation. If a model potential in the empirical approach is modified to partially include electronic effects, then the approach is usually called semiempirical. Success in first-principles calculations is limited by the availability of computer resources. Empirical approaches, on the other hand, are readily applied to systems with large numbers of particles.

Empirical pair potentials (EPP's) suffer from many problems¹⁻²³ (at least in the case of metals): (a) $C_{11} - C_{12} = 0$, where C_{11} and C_{12} are elastic constants, (b) the vacancy formation energy is equal to the cohesive energy, (c) the surface relaxation is outward and reconstruction is not predicted, contrary to experimental observations, (d) the change in the entropy at the melting point is

overestimated, (e) the melting point is also overestimated, and, finally, (f) the EPP approach does not include many-body effects.

In order to overcome some or all of the shortcomings of the EPP approach, several semiempirical methods have been developed, such as the embedded-atom method (EAM),¹⁻¹⁹ effective-medium theory (EMT),^{20,21} tight-binding method,²² and glue model.²³ Of these methods, the EAM has been shown to be quite successful in predicting many properties of single as well as multicomponent systems in the solid state and is also simple enough for use in computer simulations. The appeal of the EAM is that it uses simple analytical functions in the calculation of the energy of a system of particles; contrary to empirical approaches, the EAM imposes conditions on such functions so that a host of equilibrium bulk properties are reproduced. Since the EAM functions are built to reproduce bulk properties of a perfect, infinitely extended solid at $T = 0$ K, it is not clear, *a priori*, whether this method will yield predictions in agreement with experimental results when it is applied to calculate properties of solids at high temperature and for defected crystals (such as those having a free surface). Restricting our attention to the behavior of surfaces at high temperatures, EAM functions have recently been used in molecular-dynamics calculations to study the disordering and melting of the Cu(110) and Ni(110) surfaces.¹² Premelting effects and anisotropy in the diffusion of atoms in the top layers were observed in those studies.¹²

One of the most studied systems in recent years has been the (110) surface of lead. Experimental results, obtained with different techniques,²⁴⁻²⁶ indicate that the (110) surface of Pb disorders and then melts at temperatures considerable lower than the bulk melting tempera-

ture ($T_m = 600$ K). As T_m is approached from below, more and more layers become “liquidlike,” although some order is preserved in this “quasiliquid” layer due to the presence of order in the yet unmelted substrate layers. Anisotropic diffusion of lead adatoms on the (110) surface has also been observed.²⁶ Furthermore, theoretical support for an anisotropy in the long-range order on the Pb(110) surface has been given recently.²⁴ In passing, we note that not all low-index surfaces of metals are expected to exhibit this type of behavior. In fact, surfaces vicinal to the Pb(110) surface, which are more compact and stable than the (110), do not show any premelting behavior.^{23–26} A preliminary study of the Pb(110) surface using molecular-dynamics (MD) and EAM functions has been given elsewhere.¹⁶ The results of that simulation showed a sharp decline of the inplane structure factor of the top layers and the creation of adatoms on top of the first layer at temperatures considerably below the bulk melting point. However, in that study disordering was observed to proceed in the bulk slower than expected. In particular, a simulation run at 650 K for 100 psec failed to show complete bulk melting. The objective of the present study is to use the EAM functions for Pb to calculate properties associated with the formation and migration of defects in the surface region. The present calculations of energetics of defect formation and migration (at 0 K) and the Debye surface temperature should nonetheless be relevant for the interpretation of recent experimental studies of disordering, adatom diffusion, and melting of low-index faces of metals.

In Sec. II we review the salient features of the EAM and give details on the calculation procedures used in this work. Results are presented in Sec. III, first for processes of diffusion in the bulk and then for the energetics of defect motion at the surface. In Sec. IV, our results for the activation energies of motion of various types of defects through the bulk or on the surface are compared with available experimental data or with results of calculations for other systems.

II. EMBEDDED-ATOM METHOD AND ITS APPLICATIONS

The embedded-atom method, a semiempirical method developed by Daw and Baskes,¹ is an appropriate framework for the calculation of interatomic interactions in a metallic environment. The EAM has been discussed in detail in the literature;^{1–19} therefore, only highlights of the method are presented here.

In the EAM, a volume-dependent term, usually referred to as the embedding function, is added to a pair potential. Justification for this volume-dependent term is attributed to nonlocal electrons of metals. The embedding term is a function of the electronic charge density and constitutes the major contribution to the cohesive energy of each atom. The energy of atom i can then be written as

$$E_i = \frac{1}{2} \sum_{j \neq i} \varphi_{ij} + F_i(\rho_i), \quad (1)$$

where E_i is the energy of atom i , φ_{ij} is the two-body elec-

trostatic potential between cores of atoms i and j , F_i is the embedding energy of atom i , and ρ_i is the charge density at site i due to all of the other atoms except the one at site i . In practice, functional forms are considered for E_i , φ_{ij} , and F_i and their parameters are determined by fitting to the experimental bulk properties of metals such as the lattice constant, cohesive energy, bulk modulus, shear modulus, vacancy formation energy, etc. Details of the calculations of the EAM functions are described in Ref. 18. The EAM has been applied successfully to bulk-related problems, such as the calculation of elastic properties, diffusion,^{6,8} phonon-dispersion curves,^{4,19} Gibb's free energy,⁷ liquid properties,⁵ grain boundaries,⁷ defect properties,⁸ alloy properties,¹⁷ and vacancies and interstitials.⁸ The ability of the EAM to accurately characterize properties of metals is its strongest justification. More recently, the EAM has been applied, with various degrees of success, to calculations of surface properties such as structure,⁵ relaxation,^{3,19} reconstruction,³ phonons,¹⁰ energy,^{3,12} and adatom diffusion.^{9,33}

In our MD simulations, the classical equations of motion are integrated (numerically) for all atoms in the system using the EAM to approximate the force that is experienced by each atom. Values of the velocities and positions of the particles at any time are calculated using an iterative approach based on the Nordsieck algorithm.²⁸

In the traditional MD simulation, the energy E , volume V , and number of particles N are kept constant. Therefore, the time average of any physical quantity in the constant E, V, N mode is equal to the microcanonical ensemble average at that energy (ergodicity). In order for the ergodicity condition to be satisfied, i.e., time average equal to the ensemble average, one has to make sure that the simulation propagates long enough in time that E is conserved within a reasonable fluctuation. Averages over a canonical ensemble where N, V, T are constant, or as isothermal-isobaric ensemble where N, P, T are constant, are more easily compared with the experimental results. Calculations of interatomic forces in the MD simulation usually take about 80% of the total simulation time. When all particles interact with one another, i.e., each particle interacts with all the remaining $N - 1$ particles, $N(N - 1)/2 = O(N^2)$, calls to the force subroutine are made. On the other hand, if a cutoff distance is considered for the interatomic forces, then each particle will interact with only its N_n neighbors within the cutoff range. The total calls to the force subroutine will, therefore, reduce to $N \times N_n = O(N)$. In our MD simulation, a cutoff radius $r_c = 6.48$ Å, which is approximately midway between the third and fourth nearest neighbors, has been used. The EAM functions are smoothed near the cutoff using the procedure presented by Baskes and co-workers.¹

For the calculations performed in this paper, we have used the EAM functions developed by Karimi *et al.*¹⁸ For the calculations of surface properties, a slab of 20 layers with 70 atoms per layer was used. Periodic boundary conditions were imposed parallel to the planes, i.e., in the x and y directions. For the calculations of bulk properties, a cubic computational box of atoms with periodic

boundary conditions in all three directions were employed. For the surface calculations, our MD simulation was propagated for a period of 700 ps near the melting temperature of lead. MD was first propagated for 600 ps in isothermal, isobaric ensemble followed by a 100-ps run in a microcanonical ensemble. Averages were taken over the last 100-ps run. For temperatures below the melting temperature or for a smaller system, shorter runs were performed.

Calculations at 0 K were performed using molecular statics (MS), which is based on the conjugate gradient technique.²⁹ In the MS used here, atoms are moved opposite to their respective gradients so as to minimize the total energy of the system. One should realize that the system might sit in a local minima rather than a global minimum; therefore, there is no guarantee that the final state of the system will be the global minimum. One possible check is to disturb the system from its local minimum and perform a MS run. The final state may be lower in energy than the restart state. Another way of seeking the global minimum is by using MD. Different initial configurations are considered and a MD simulation is performed at finite temperature and propagated to 0 K. If the final configuration happens to be the global minimum of the system then MD should converge to the same final configuration regardless of the initial configurations or simulated annealing procedure. Calculations at finite temperatures are carried out using the MD simulation; however, it should be noted that such calculations are computationally more expensive. Considering the fact that some of the physical quantities are only weakly temperature dependent, the use of MS-related techniques is well justified.

III. RESULTS

A. Diffusion at near surface and in bulk

In this section, we present our results for the energetics of defects in the bulk and in a region near the surface.

We have first constructed a model of bulk solid Pb with 500 atoms and periodic boundary conditions in all three directions. Using our MS code, we have calculated the average energy per atom in the bulk E_c . Using Eq. (6), we have also calculated the single-vacancy formation energy $E_{1v}^f = 0.500$ eV for generation of a single vacancy in the bulk. The fact that our values of -2.036 and 0.500 eV for E_c and E_{1v}^f are in good agreement with the experimental values²⁷ of -2.04 and 0.498 eV, respectively, reflect the fact that our EAM functions are fitted to the bulk properties including E_c and E_{1v}^f . We have then used our slab of 20 layers with 70 atoms per layer to do the near-surface simulations. We then calculated the average energy per atom in each layer $E(l)$ (Table I). Next, we calculated the vacancy formation energies for creation of a vacancy in different layers $E_{1v}^f(l)$, and energy for creation of an adatom and a vacancy in layer l , $E_{1v}^f(l) + E_{1a}^f$, with the adatom and vacancy uncorrelated. It should be noted that in the calculation of E_{1v}^f , relaxation has already been included. Finally, we calculated the adatom formation energy, $E_{1a}^f = 0.099$ eV. Notice

TABLE I. $E(l)$ is the average energy of each atom in layer l , E_{1v}^f [see Eq. (6)] is the formation energy of a vacancy in layer l , $E_{1a}^f = 0.099$ eV [see Eq. (7)] is an adatom formation energy, $E_{1v}^f(l) + E_{1a}^f$ [see Eqs. (6) and (7)] is the energy for creation of an adatom and a vacancy in layer l with adatom and vacancy isolated from one another, and $l = 1$ is the topmost layer. All energies are in eV.

l	$E(l)$	$E_{1v}^f(l)$	$E_{1v}^f(l) + E_{1a}^f$
1	-1.793	0.093	0.192
2	-1.984	0.480	0.579
3	-2.036	0.490	0.589
4	-2.036	0.491	0.590
5	-2.036	0.499	0.598
bulk	-2.036	0.500	0.599

the rapid convergence to bulk values after just a few layers. A similar trend has been observed in simulations of other (110) surfaces.¹²

From Table I and the following formula

$$E_{\text{surf}} = \sum_l [E(l) - E_c], \quad (2)$$

we can easily calculate the surface energy. Our value of $E_{\text{surf}} = 0.293/\text{atom}$ or 275 ergs/cm^2 is much smaller than the value of $500\text{--}600 \text{ ergs/cm}^2$ obtained from measurements of the liquid-vapor surface energy and extrapolated to $T = 0 \text{ K}$.³⁶ Although our calculated surface energy value is about $45\text{--}55\%$ smaller than the experimental values (which are averages over several faces), it is still consistent with other EAM calculations which all underestimate the surface energy.^{6,33} A recent calculation using the modified EAM (Ref. 1) has reported a value of 431 ergs/cm^2 for the (110) surface energy of Pb.

We calculated the energies for formation of a diadatom (E_{2a}^f) and divacancy [$E_{2v}^f(l, l')$] in different layers. $E_{2v}^f(l, l')$ is the formation energy for creating two vacancies in the layer l separated from one another by a nearest-neighbor distance. The slab described in the previous section is modified by adding two nearest-neighbor adatoms on its surface or by creating two nearest-neighbor vacancies in the layer l . Using our MS code and equations similar to (6) and (7), we calculated E_{2a}^f and $E_{2v}^f(l, l')$ (Table II).

Finally, we would like to discuss the calculations of bulk single-vacancy (E_{1v}^m) and divacancy migration ener-

TABLE II. $E_{2v}^f(l, l')$ is the divacancy formation energy, $E_{2a}^f = 0.067$ eV is the diadatom formation energy, and $E_{2v}^f(l, l') + E_{2a}^f$ is the formation energy of a divacancy diadatom pair. All energies are in eV.

l, l'	$E_{2v}^f(l, l')$	$E_{2v}^f(l, l') + E_{2a}^f$
1,1	0.083	0.15
2,2	0.947	1.014
3,3	0.200	0.267
4,4	0.921	0.988
5,5	0.928	0.995
bulk	0.941	1.008

gies, and self-interstitial migration energies. We created a vacancy in the 10th layer which should be close to the bulk environment. A nearest neighbor to the vacancy along the close-packed direction is moved toward the vacancy; following a similar procedure used for a surface vacancy, we were able to calculate the migration energy of a vacancy along the close-packed direction $E_{1v}^m = 0.479$ eV. Using the single-vacancy formation energy $E_{1v}^f = 0.5$ eV, calculated in the previous section, we can determine the monovacancy activation energy $E_d = 0.5 + 0.479 = 0.979$ eV. This is in very good agreement with the prediction of an Arrhenius form fit to the experimental data $E_d = 1$ eV.²⁷ Using a similar approach, we tried to calculate the migration energy of a vacancy to the next-nearest neighbor site along the close-packed direction. Instead, we noticed an exchange mechanism in which a nearest neighbor to the vacancy along the close-packed direction is pushed toward the vacancy; the lattice site so vacated is filled by the next-nearest-neighbor atom. The migration energy for this exchange mechanism is about $E_{1v}^m = 0.485$ eV.

The calculation of the divacancy binding energy proceeds as follows. Two vacancies are created in the bulk region of our slab and the binding energies of these two vacancies are calculated as a function of their separation distance from the following formula:^{8,24}

$$E_B = 2E_{1v}^f - E_{2v}^f. \quad (3)$$

Our results for E_B are presented in Table III. From Table III, we see that two vacancies are bound together stronger when they are 1NN of one another than the further separated pairs (NN denotes nearest neighbor). For this reason and the fact that in the fcc structure there exist atoms which are nearest neighbors to both vacancies (see Fig. 1), the diffusion of a 1NN divacancy may occur by diffusion of one of the vacancies toward the 1NN atom.

We calculate self-interstitial formation and migration energies at different sites. At high temperatures, diffusion may be the result of a dissociative mechanism. In such a case, an atom jumps from its lattice site into an interstitial site leaving behind a vacant lattice site. The interstitial atom hops from one interstitial site to another until it eventually finds a vacant lattice site to fill. Therefore, the distance that a self-interstitial atom travels is proportional to the vacancy concentration. To calculate the self-interstitial formation energy, an interstitial is added along the close-packed direction in the bulk region of our slab and its formation energy is calculated to be $E_{int}^f = 1.347$

TABLE III. E_B is the binding energy (in eV) between the two vacancies when vacancies are 1NN, 2NN, 3NN, and 4NN of one another.

Configuration	E_B
1NN	0.07
2NN	0.009
3NN	0.007
4NN	0.007

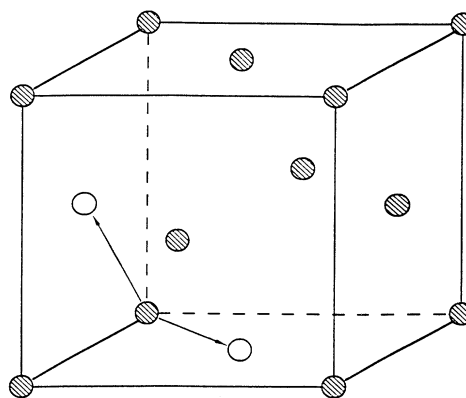


FIG. 1. Various moves of a lead atom on a Pb(110) surface. Moves (1) and (3) correspond to the motion of a lead adatom parallel and perpendicular to a trough while move (2) corresponds to the motion of an adatom in a direction between the parallel and perpendicular directions.

eV. Using the value of 0.5 eV for the single-vacancy formation energy in the bulk one can easily calculate the formation energy for a Frenkel pair to be $E_{int}^f + E_{1v}^f = 1.347 + 0.5 = 1.847$ eV. Using a similar approach, the energy for formation of a Frenkel pair across the close-packed direction is given to be $E_{int}^f + E_{1v}^f = 2.171 + 0.5 = 2.681$ eV. We have also calculated the migration energy of an interstitial along different paths. Our calculations predict that the [100] split interstitial is the most stable interstitial (lowest in energy). This is consistent with the experiment and other EAM calculations.^{3,18} If we try to move it along any other direction, it reverts to the [100], [010], or [001] direction. The migration energy of the self-interstitial dumbbell along [100] to [010] directions is $E_{int}^m = 0.1$ eV. At higher temperatures diffusion by dissociative mechanism (where an atom moves from its regular site to an interstitial site leaving behind a vacancy⁸) might be dominant. The total activation energy for diffusion by a dissociative mechanism E_{dis} can then be calculated along the [110] direction, giving a value of $E_{dis} = 1.347 + 0.123 = 1.47$ eV. Another mechanism of high-temperature diffusion is due to monovacancy jumps to the next-nearest neighbors. However, in our calculation, we have not seen any evidence for this kind of mechanism. We tried to migrate a vacancy to its second-nearest neighbor by migrating its second-nearest-neighbor atom toward it. However, during the process of approaching the atom toward the vacancy it is exchanged by its first-nearest-neighbor atom. This indicates that the migration energy for monovacancy jumps to the next-nearest-neighbor sites is higher than the one for the exchange mechanism.

B. Diffusion at surfaces

The activation energy for diffusion of an adatom on a Pb(110) surface is studied with an adatom sitting in an adsorption site. Some possible moves that an adatom can

make are displayed in Fig. 2. In moves 1 or 2, the adatom moves along or across the closed-packed direction. In move 3, which is usually referred to as a concerted move, two atoms (*a* and *b*) are involved in the move and each atom moves along the main diagonal of the surface unit cell.

Using MS and the slab described in the previous section, we calculated migration energies for these different moves. For the calculation of the migration energy, the adatom is moved through the desired path and is allowed to relax in the plane perpendicular to the path. All the other atoms around the adatom are allowed to relax in all three directions. The adatom migration energy can then be calculated from the following formula:

$$E_a^m = E_{\text{sad}} - E_0, \quad (4)$$

where E_0 is the total energy of the system including the adatom after relaxation and E_{sad} is the saddle-point energy of the system which is usually the energy when the adatom is near the bridge site. Our results for the adatom migration energies along and across the close-packed directions are 0.215 and 0.454 eV, respectively. To our knowledge, no experimental data for migration energies of an adatom along these paths are available; however, the activation energy of self-diffusion of lead on the Pb(110) surface across the channel is reported in Ref. 26 to be $E_d = 1.0$ eV. From the surface single-vacancy formation energy calculated in the next section, one can easily calculate the activation energy for the self-diffusion of a surface atom across the close-packed direction to be equal to $E_d = 0.547$ eV, which is about 45% lower than experimental value. Using the same method, we calculated the migration energy for the move along the 3 direction. In fact, we noticed the exchange of the adatom with its nearest-neighbor atom along the path. Our result for

the migration energy of the concerted move is 0.45 eV. From our results, it is evident that diffusion of a Pb atom in a Pb(110) surface is quite anisotropic and diffusion along the troughs is preferred. It should be noted that this anisotropy has been detected experimentally and predicted theoretically (see previous section); however, because of the limitations of the techniques used, atom beam scattering and ion channeling, it was not possible to obtain a quantitative determination of activation energies. Diffusion by concerted moves has been predicted theoretically^{9,14,15,30-33} and recently observed in field-ion-microscope experiments of Kellogg-Feibelman³⁴ and Chen-Tsong³⁵ on Pt(001), and Ir(001), Ni surfaces. A recent calculation for low-index copper surfaces using the effective-medium theory shows that diffusion by an exchange mechanism is in fact important for Cu(100) and Cu(110) and has an activation energy of 0.23 eV, which is between those along and across the troughs.³¹ A recent helium beam scattering experiment found an activation energy for self-diffusion of 0.28 eV on Cu(001).¹⁷ A similar calculation for diffusion of an Au adatom on an Au(110) surface using EAM (Ref. 9) predicts values of 0.27, 1.16, and 0.35 eV for direct (along and across the troughs) and concerted moves, respectively.

In this part, we discuss the calculation of the migration energy of a single vacancy in a Pb(110) surface. A vacancy is created in the center of one of the free surfaces of the slab described in the previous section. The nearest surface atom to the vacancy is then moved toward the vacancy along the close-packed direction. The moving atom is allowed to relax in the plane perpendicular to the close-packed direction. All the other atoms are also allowed to relax in all three directions. We calculated the vacancy migration energy using a formula similar to Eq. (4),

$$E_v^m = E_{\text{sad}} - E_0, \quad (5)$$

where E_0 is the relaxed energy of the system with one vacancy at the surface and E_{sad} is the saddle-point energy which is usually the energy of the system when the moving atom is near halfway between its initial position and the vacancy. Our results for vacancy migration energies along and across the close-packed direction are 0.329 and 0.382 eV, respectively, thus indicating that the vacancy migration energy on the Pb(110) surface is weakly anisotropic. Based on our results for adatom and surface vacancy migration energies, we conclude that diffusion along the close-packed direction is dominated by adatoms, while diffusion across the close-packed direction is dominated by vacancies.

We turn now to the calculation of adatom and vacancy formation energies on a Pb(110) surface.

The single-vacancy formation energy (with respect to a lattice without vacancy) is defined by the formula

$$E_{1v}^f = E(N-1, 1) - E(N, 0) - E_S, \quad (6)$$

where $E(N-1, 1)$ is the energy of the solid containing $N-1$ atoms and one vacancy, $E(N, 0)$ is the energy of the perfect solid containing N atoms with no vacancies, and $E_S (> 0)$ is the sublimation energy which is the nega-

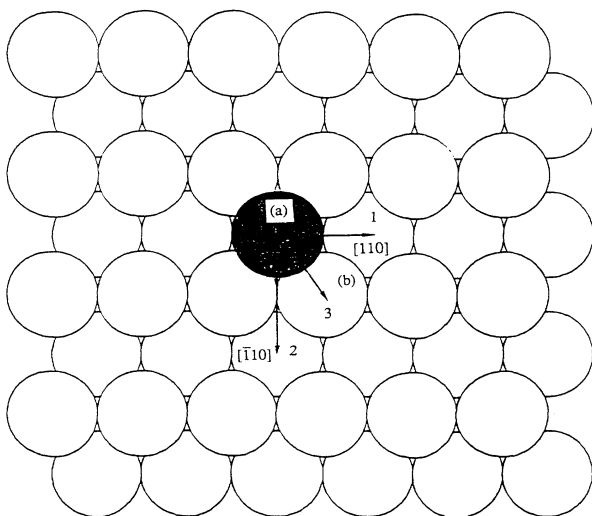


FIG. 2. Divacancy in a fcc lattice. The filled circles are atoms, the empty circles are 1NN vacancies. The arrows show the migration paths of a divacancy.

tive of the average energy of bulk atoms. Our result for the single-vacancy formation energy is $E_{1v}^f = 0.093$ eV. To our knowledge there is no experimental data for E_{1v}^f in the surface region. However, our E_{1v}^f for the surface can be compared with the experimental value of $E_{1v}^f = 0.49$ eV of the bulk region. It is quite reasonable to expect that E_{1v}^f for the surface be smaller than E_{1v}^f for the bulk.¹⁴ This is, in fact, related to the weak binding energy of atoms of open, unreconstructed surfaces as compared with that in the bulk region.

The adatom formation energy on the surface of the metal is defined by

$$E_{1a}^f = E(N+1, 1) - E(N, 0) + E_S, \quad (7)$$

where $E(N+1, 1)$ is the energy of the solid containing $N+1$ atom and one adatom. Our calculated value of E_{1a}^f is 0.099 eV. It has been shown in simulations of the dynamics of (110) surfaces that adatom formation and creation of vacancies in the top layer promote disordering affecting several layers.^{12, 16, 21}

C. Surface Debye temperature

Disordering at lower temperature is mostly due to lattice vibrations. Using a Debye model at low temperature, the attenuation of the intensities of Bragg diffraction peaks is given by

$$\ln|S_l|^2 = -3\hbar^2 |g|^2 T / (mk_B \theta_D^2), \quad (8)$$

where S_l is the structure factor of layer l , \hbar is the Planck's constant, g is a two-dimensional reciprocal-lattice vector in layer l , T is the temperature, m is the mass of the lead atom, k_B is the Boltzmann constant, and θ_D is the Debye temperature of layer l . From our MD simulation, we calculated $|S_l|^2$ at the temperature $T = 300$ K and along two different g vectors along and across the close-packed direction. By substituting $|S_l|^2$ in Eq. (8) we find the surface Debye temperature of lead to be $\theta_{DS} = 67$ K, which is about 35% lower than the bulk value of $\theta_{DB} = 103$ K.²⁷ This is consistent with the "rule of thumb" that says $\theta_{DS} \sim (\frac{2}{3})\theta_{DB}$.³⁷ A recent MD simulation of the Al(110) surface²¹ using the EMT predicts a value of $\theta_{DS} = 250$ K for that surface²² which is about 38% lower than the bulk value. Our surface Debye temperature is in good agreement with the prediction of a simple model developed in Ref. 37 which gives $\theta_D = 74$ K. At higher temperatures lattice vibrations are no longer harmonic and nonlinear terms should be added to Eq. (8).

IV. DISCUSSION AND SUMMARY

In this work, we used MD and MS simulations to calculate the energetics of various processes of atoms and vacancies moving at the surface as well as in the bulk. Various mechanisms of disordering have been considered. In particular, we have calculated migration and formation energies of an adatom migrating along three direc-

tions (along and across the close-packed directions, and along the diagonal of the surface unit cell). From our results, it is concluded that an adatom feels the lowest-energy barrier while moving along the close-packed direction (in the trough), the highest while moving across the close-packed direction, and an intermediate value for the energy barrier while moving along the surface unit-cell diagonal. In the latter case an exchange mechanism is involved. Other important quantities which were calculated include: (1) formation and migration energies of single vacancy (E_{1v}^f), divacancy (E_{2v}^f), adatom (E_{1a}^f), and diadatom (E_{2a}^f) at the surface. As expected, the absolute values of these energies are much lower than for "harder," higher melting-point surfaces, such as the (110) surfaces of Cu and Ni.¹² However, for lead, the vacancy formation energy for the first layer is a smaller fraction of the bulk vacancy energy than for the case of Cu or Ni. This suggests that premelting effects are relatively stronger in Pb than Cu or Ni, as observed. (2) Formation and migration energies of creating a single vacancy or divacancy in different layers. (3) Formation energies of an adatom-monovacancy (first layer) and diadatom divacancy (first layer). Our results indicate that the energy of creating a diadatom divacancy is smaller than that for creating a single adatom single vacancy. This point is also confirmed by formation of adatom clusters. (4) Surface energy of Pb(110); our value is 275 ergs/cm², lower than the experimental value³⁶ of 500–600 ergs/cm², but consistent with the trend displayed in other EAM calculations. (5) Surface Debye temperature of Pb(110); our value, $\theta_D = 67$ K, is in good agreement with the value of 74 K estimated in Ref. 37.

In conclusion, our calculations give a fairly complete picture of the energetics of diffusion at the Pb(110) surface which should be useful to experimental and other computer simulations. The trends observed in simulations of (110) surfaces of other metals have been confirmed. As expected, the EAM underestimates the surface energy. The ever increasing number of experiments probing the (110) surface of lead should soon give us more stringent bounds for the values of the energetics calculated in this present work.

ACKNOWLEDGMENTS

This research was sponsored in part by the Division of Materials Sciences, U.S. Department of Energy under Contract No. DE-AC05-84OR21400 with Martin Marietta Energy Systems, Inc., and one of the authors (M.K.) obtained support from Oak Ridge Associated Universities. We wish to thank Dr. Murray Daw and Dr. Steven Foiles for sharing their MD code and for helpful discussions, and the Pittsburgh Supercomputer for Cray time. We would like to thank Dr. Mark Mostoller of the Oak Ridge National Laboratory for critical review of the manuscript and Dr. Stanley Sobolewski for technical help. We acknowledge Dr. Frank Six of the MSFC, Gerald Karr of the UAH, and support from NASA.

- ¹M. S. Daw and M. I. Baskes, *Phys. Rev. B* **29**, 6443 (1984); *Phys. Rev. Lett.* **50**, 1285 (1983); M. I. Baskes, J. S. Nelson, and A. F. Wright, *Phys. Rev. B* **40**, 6085 (1985); M. I. Baskes, *ibid.* **46**, 2727 (1992).
- ²S. M. Foiles and M. S. Daw, *Phys. Rev. B* **38**, 12 643 (1988).
- ³S. M. Foiles, M. I. Baskes, and M. S. Daw, *Phys. Rev. B* **33**, 7983 (1986); S. P. Chen and A. F. Voter, *Surf. Sci.* **244**, L107 (1991).
- ⁴M. S. Daw and R. D. Hatcher, *Solid State Commun.* **56**, 697 (1985).
- ⁵S. M. Foiles, *Phys. Rev. B* **32**, 3409 (1985); M. S. Daw and S. M. Foiles, *Phys. Rev. Lett.* **59**, 2756 (1987).
- ⁶J. B. Adams, S. M. Foiles, and W. G. Wolfer, *J. Mater. Res.* **4**, 102 (1989); J. B. Adams and W. G. Wolfer, *J. Nucl. Mater.* **158**, 25 (1988); C. L. Liu, J. M. Cohen, J. B. Adams, and A. F. Voter, *Surf. Sci.* **253**, 334 (1991).
- ⁷S. M. Foiles and J. B. Adams, *Phys. Rev. B* **40**, 5909 (1989).
- ⁸J. B. Adams and S. M. Foiles, *Phys. Rev. B* **41**, 3316 (1990); R. A. Johnson, *Philos. Mag. A* **63**, 865 (1991).
- ⁹L. D. Roelofs, J. I. Martin, and R. Sheth, *Surf. Sci.* **250**, 17 (1991).
- ¹⁰J. S. Nelson, E. C. Sowa, and M. S. Daw, *Phys. Rev. Lett.* **61**, 1977 (1988).
- ¹¹M. S. Daw and S. M. Foiles, *J. Vac. Sci. Technol. A* **4**, 1412 (1986).
- ¹²R. N. Barnett and Uzi Landman, *Phys. Rev. B* **44**, 3226 (1991); E. T. Chen, R. N. Barnett, and Uzi Landman, *ibid.* **41**, 439 (1990).
- ¹³J. B. Adams, W. G. Wolfer, and S. M. Foiles, *Phys. Rev. B* **40**, 9479 (1989).
- ¹⁴C. L. Liu and J. B. Adams, *Surf. Sci.* **265**, 262 (1992); E. A. Colbourn, *Surf. Sci. Rep.* **15** (1992).
- ¹⁵G. L. Kellogg, A. F. Wright, and M. S. Daw, *J. Vac. Sci. Technol. A* **9**, 1757 (1991).
- ¹⁶P. Tibbets, M. Karimi, D. Ila, I. Dalins, and G. Vidali, *J. Vac. Sci. Technol. A* **9**, 1937 (1991).
- ¹⁷H.-J. Ernst, F. Fobre, and J. Lapujoulade, *Phys. Rev. B* **46**, 1929 (1992); Y. Liu and P. Wynblatt, *Surf. Sci.* **240**, 245 (1990); **241**, L21 (1991).
- ¹⁸M. Karimi, Z. Yang, P. Tibbets, D. Ila, I. Dalins, and G. Vidali, in *Atomic Scale Calculations of Structure in Materials*, edited by M. S. Daw and M. A. Schluter, MRS Symposia Proceedings No. 193 (Materials Research Society, Pittsburgh, 1980), p. 83; R. A. Johnson, *Phys. Rev. B* **37**, 3924 (1988); D. J. Oh and R. A. Johnson, *J. Mater. Res.* **3**, 471 (1988).
- ¹⁹M. Karimi and M. Mostoller, *Phys. Rev. B* **45**, 6289 (1992).
- ²⁰K. W. Jacobsen, J. K. Nørskov, and M. J. Puska, *Phys. Rev. B* **35**, 7423 (1987).
- ²¹P. Stoltze, *J. Chem. Phys.* **92**, 6306 (1990).
- ²²M. W. Finnis and J. E. Sinclair, *Philos. Mag. A* **50**, 45 (1986); **53**, 161(E) (1986).
- ²³F. Ercolessi, M. Parrinello, and E. Tosatti, *Philos. Mag. A* **58**, 213 (1988).
- ²⁴A. W. D. van der Gon, H. M. van Pinxteren, J. W. M. Frenken, and J. F. van der Veen, *Surf. Sci.* **244**, 259 (1991); R. Lipowsky, U. Breuer, K. C. Prince, and H. P. Bouzel, *Phys. Rev. Lett.* **62**, 913 (1989); H. Löwen, *ibid.* **64**, 2104 (1990).
- ²⁵J. W. M. Frenken and J. F. van der Veen, *Phys. Rev. Lett.* **54**, 134 (1985); K. C. Prince, U. Breuer, and H. P. Bonzel, *ibid.* **60**, 1146 (1988); J. W. M. Frenken, J. P. Toennies, and Ch. Wöll, *ibid.* **60**, 1727 (1988).
- ²⁶J. W. M. Frenken, B. J. Hinch, J. P. Toennies, and Ch. Wöll, *Phys. Rev. B* **41**, 938 (1990).
- ²⁷R. Yamamoto and M. Doyama, *Phys. Rev. B* **8**, 2586 (1973); C. Kittel, *Introduction to Solid State Physics*, 5th ed. (Wiley, New York, 1976); M. A. Omar, *Elementary Solid State Physics* (Addison-Wesley, Reading, MA, 1974).
- ²⁸A. Nordsieck, *Math. Comp.* **16**, 22 (1962).
- ²⁹R. Fletcher and C. M. Reeves, *Comput. J.* **7**, 149 (1964).
- ³⁰P. J. Feibelman, *Phys. Rev. Lett.* **65**, 729 (1990).
- ³¹L. Hansen, P. Stoltze, K. W. Jacobsen, and J. K. Nørskov, *Phys. Rev. B* **44**, 6523 (1991).
- ³²D. W. Bassett and P. R. Webber, *Surf. Sci.* **70**, 520 (1978); J. D. Wrigley and G. Ehrlich, *Phys. Rev. Lett.* **44**, 661 (1980).
- ³³C. L. Liu, J. M. Cohen, J. B. Adams, and A. F. Voter, *Surf. Sci.* **253**, 334 (1991).
- ³⁴G. L. Kellogg and P. J. Feibelman, *Phys. Rev. Lett.* **64**, 3143 (1990); G. L. Kellogg, *Surf. Sci.* **266**, 18 (1992).
- ³⁵C. Chen and T. T. Tsong, *Phys. Rev. Lett.* **64**, 3147 (1990).
- ³⁶W. R. Tyson and W. A. Miller, *Surf. Sci.* **62**, 267 (1977); J. A. Alonso and N. H. March, *Electrons in Metals and Alloys* (Academic, New York, 1989).
- ³⁷F. C. M. J. M. Van Delft, *Surf. Sci.* **251/252**, 690 (1991).